Composites Communications 6 (2017) 59–62

Contents lists available at ScienceDirect

Composites Communications

journal homepage: www.elsevier.com/locate/coco

Mechanical behaviour of photovoltaic composite structures: Influence of geometric dimensions and material properties on the eigenfrequencies of mechanical vibrations

M. Aßmus*, K. Naumenko, H. Altenbach

Chair of Engineering Mechanics, Institute of Mechanics, Faculty of Mechanical Engineering, Otto von Guericke University Magdeburg, Universitätsplatz 2, 39106 Magdeburg, Germany

ARTICLE INFO

Keywords:
Photovoltaic module
Geometry
Materials
Structural dynamics
Layerwise theory
Finite element analysis

ABSTRACT

During service and transportation, photovoltaic modules are subjected to dynamic excitation, too. From the viewpoint of structural engineering, natural frequencies of such structures should be outside of the stimulus spectrum. Knowing the location of the natural frequencies is therefore essential. The present contribution is the continuation of a recently published paper, where the considerations were stipulated on statics, while directions to optimal geometric and material parameters were revealed. In addition, we enlarge our framework and investigate the eigenbehaviour of different layouts. Thereby, we make use of an efficient and effective approach to computational solutions based on the extended layerwise theory. The results presented here constitute characteristic indexes useful in conceptual and design phase for dimensioning and material selection of photovoltaic modules.

1. Introduction

1.1. Motivation

The durability and operational reliability of photovoltaic modules are essentially influenced by the mechanical design of components involved. Restricting to terrestrial photovoltaic modules, the components available on the market are subject to a large variability of mechanical properties and geometric dimensions. As visualised in Fig. 1, this affects mainly the front and back cover (≙ skin layers) as well as the core layer. It is possible to extract significant ratios of these constituents, which we will directly recapitulate from [1]. Subsequent ranges for geometric ratios

$$TR = \frac{h^c}{h^t + h^b} \approx 0.125...0.45 \tag{1}$$

$$LR = \frac{L_2}{L_1} \approx 0.25...1 \tag{2}$$

$$TLR = \frac{H}{L_{\min}} \approx 2 \times 10^{-3}...1.4 \times 10^{-2} \tag{3}$$

and the following range for the shear modulus ratio are known.

$$GR = \frac{G^c}{G^s} \approx 7 \times 10^{-6}...1.5 \times 10^{-2} \tag{4}$$

Herein, we consider isotropic materials, so $G = \frac{E}{2(1+\nu)}$ holds true where E is YOUNG's modulus and ν is POISSON's ratio. Furthermore, we introduce the mass density ratio with subsequent range assumed.

$$MDR = \frac{\rho^c}{\rho^s} \approx 4 \times 10^{-2}...1 \tag{5}$$

The conscious choice of these parameters is directly related to stiffness, strength, and reliability of photovoltaic modules.

In a preceding publication [1], we have concentrated on the static deflection behaviour of such structures. In the present contribution, we focus on the eigenbehaviour solely, since the location of natural frequencies is crucial in the context of reliability as reported in [2]. Experimental analysis on structural dynamics of photovoltaic modules can be found in [3–7]. Since experiments are usually elaborate and expensive, numerical estimations are beneficial.

Due to the slenderness of photovoltaic modules, cf. Eq. (3) ($L_1 \approx L_2 \gg H$), it is reasonable to make use of the mechanics of thin-walled structures, whereby individual layers should be considered. The different approaches are discussed in [8], while it turns out that the extended layerwise theory (XLWT) originally proposed in [9] has the highest potential to application. Within this approach, a homogeneity

* Corresponding author.
E-mail address: marcus.assmus@ovgu.de (M. Aßmus).

http://dx.doi.org/10.1016/j.coco.2017.10.003
Received 5 July 2017; Received in revised form 2 August 2017; Accepted 21 October 2017

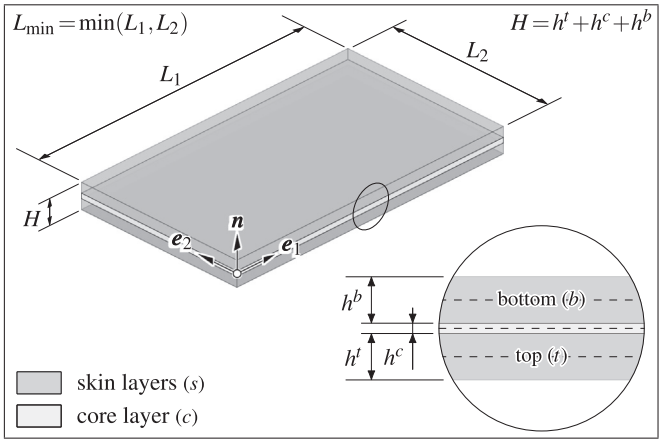

Fig. 1. Photovoltaic module composition for global structural analysis [1].

postulate is introduced for the core layer, what enables to neglect the solar cells and to reduce the mechanics to a three-layered composite. Thereby, the low transverse shear stiffness of the core layer is taken into account. The concept is approved in [10]. A numerical solution strategy by using the Finite Element Method is introduced in [11], while excessive applications can be found in [12]. In the present context, the balance equations are enriched by the terms of inertia and the numerical solution strategy is expanded correspondingly to solve eigenproblems. However, the variation of geometric dimensions and material parameters is still in the foreground to reveal directions to optima with respect to above introduced ratios.

1.2. Frame of Reference

The XLWT is based on the theory of elastic surfaces. Here, we reduce our concern to coplanarity of all material points, i.e. initially uncurved surfaces. These surfaces comprise five degrees of freedom: two in-plane translational ($\boldsymbol{a} = a_1\boldsymbol{e}_1 + a_2\boldsymbol{e}_2$), one out-of-plane translational (w), and two out-of-plane rotational ($\boldsymbol{\varphi} = \varphi_1\boldsymbol{e}_1 + \varphi_2\boldsymbol{e}_2$). In the sequel, we make use of the direct tensor notation for a rational description, whereby tensors of first, second, and fourth order are written as $\boldsymbol{b}$, $\boldsymbol{B}$, and $\mathcal{B}$. Furthermore, $\times$, $\cdot$, $:$, and $\otimes$ represent the cross product, the single contraction, the double contraction, and the dyadic product. ∇ is the nabla operator, $\nabla\boldsymbol{b}$ is the gradient of $\boldsymbol{b}$, and is the symmetric part of this gradient. Moreover, $\nabla\cdot\boldsymbol{B}$ is the divergence of $\boldsymbol{B}$. In the case of a geometrically linear theory, the deformation measures are thus $\boldsymbol{G} = \nabla^{\mathrm{sym}}\boldsymbol{a}$, $\boldsymbol{K} = \nabla^{\mathrm{sym}}\boldsymbol{\varphi}$, and $\boldsymbol{\gamma} = \nabla w + \boldsymbol{\varphi}$. The conjugate stress measures derive from a potential $W(\boldsymbol{G}, \boldsymbol{K}, \boldsymbol{\gamma})$.

$$\boldsymbol{N} = \frac{\partial W}{\partial \boldsymbol{G}} \qquad \boldsymbol{q} = \frac{\partial W}{\partial \boldsymbol{\gamma}} \qquad \boldsymbol{L} = \frac{\partial W}{\partial \boldsymbol{K}} \tag{6}$$

Therein, $\boldsymbol{N}$ is the membrane force tensor, $\boldsymbol{L}$ the polar tensor of moments, and $\boldsymbol{q}$ denotes the transverse shear force vector. Since we restrict ourselves to symmetry in transverse direction concerning the coordinate origin, the elastic potential of the uncoupled but superposed surface continuum can be derived as follows, whereby we use a description adapted from [13].

$$W(\boldsymbol{G}, \boldsymbol{K}, \boldsymbol{\gamma}) = \frac{1}{2}[\boldsymbol{G}:\mathcal{A}:\boldsymbol{G} + \boldsymbol{K}:\mathcal{D}:\boldsymbol{K} + \boldsymbol{\gamma}\cdot\boldsymbol{Z}\cdot\boldsymbol{\gamma}] \tag{7}$$

The membrane, bending, and shear stiffnesses $\mathcal{A}$, $\mathcal{D}$, and $\boldsymbol{Z}$ are given in [12] for isotropic materials. The stress measures derived fulfil the following equations of motion.

$$\nabla\cdot(\boldsymbol{N} + \boldsymbol{q}\otimes\boldsymbol{n}) + \boldsymbol{s} + p\boldsymbol{n} = \rho_\star\frac{\partial}{\partial t}[\dot{\boldsymbol{a}} + \dot{w}\boldsymbol{n} + \boldsymbol{J}_{\mathrm{T}}^{\mathrm{T}}\cdot(\boldsymbol{n}\times\dot{\boldsymbol{\varphi}})] \tag{8}$$

$$\nabla\cdot(-\boldsymbol{L}\times\boldsymbol{n}) + \boldsymbol{q}\times\boldsymbol{n} + \boldsymbol{m} = \rho_\star\frac{\partial}{\partial t}[\boldsymbol{J}_{\mathrm{T}}\cdot(\dot{\boldsymbol{a}} + \dot{w}\boldsymbol{n}) + \boldsymbol{J}_{\mathrm{R}}\cdot(\boldsymbol{n}\times\dot{\boldsymbol{\varphi}})] \tag{9}$$

The variable p denotes the out-of-plane load, while $\boldsymbol{s}$ denotes the in-plane force field, and $\boldsymbol{m}$ contains the out-of-plane moment field at the surface, cf. [12]. $\dot{\square} = \frac{\partial\square}{\partial t}$ denotes the derivative of the variable $\square$ w.r.t. time t. Therein, $\square$ is used as placeholder for tensors of arbitrary order. The right-hand side of the Eqs. (8) and (9) contain two tensors of inertia, defined as follows.

$$\boldsymbol{J}_{\mathrm{T}} = \int_h X_3\,\mathrm{d}X_3\boldsymbol{P}\times\boldsymbol{n} \tag{10}$$

$$\boldsymbol{J}_{\mathrm{R}} = \int_h X_3^2\,\mathrm{d}X_3\boldsymbol{P} \tag{11}$$

Thereby, $\boldsymbol{J}_{\mathrm{T}}$ is the tensor of translational inertia while $\boldsymbol{J}_{\mathrm{R}}$ is the tensor of rotational inertia. $\boldsymbol{P}$ is the unit tensor of the surface. Furthermore, $\rho_\star = \int_h \rho\,\mathrm{d}X_3$ is the mass density of the surface. Herein, ρ is the mass density of the material considered, while X_3 is running variable along thickness h.

Above listed equations must be considered for every layer separately, thus for skin and core layers. Thereby, kinematic constraints are introduced, cf. [9], e.g. the equality of all layer deflections at a material point. We restrict our concern to virgin materials without any imperfection at interfaces. In-plane displacements and rotations are directly coupled at these interfaces. Our description incorporates the straight line hypothesis layerwise, cf. [14]. A comprehensive description of XLWT theory can be found in [15]. The specific extensions of this theoretical framework as well as the numerical implementation will be topic of a forthcoming paper.

However, all subsequent calculations were performed with the commercial finite element code ABAQUS using a user-defined element created within the user subroutine UEL, cf. [11,15]. This framework was enlarged by incorporating inertia to enable the analyses of the eigenbehaviour. Furthermore, a parametrisation was carried out within our subroutine to allow for a simple implementation of geometry and material variations.

2. Parameter study

To attain information about the behaviour at varying structural parameters, the study is confined to the first eigenmode and therefore the first natural frequency, see Fig. 2 (bottom left). The basis for the present study is a photovoltaic module, whose geometric and material data is specified in Fig. 2 (both boxes top right). Since we restrict ourselves to a symmetric composite, $h^t \equiv h^b$, $E^t \equiv E^b$, and $\nu^t \equiv \nu^b$ hold true. The materials do not have any directional dependence. Considering the material data given, κ is the shear correction factor which is artificially introduced in $\boldsymbol{Z}$, considering the layerwise parabolic gradient of $\boldsymbol{q}$ along X_3. A moment-free support is used at all edges. The whole structure is unloaded. Details of the boundary conditions are given in Fig. 2 (bottom right). For structural analysis, the finite element developed in [11] is used for discretisation. It is a quadrilateral element with quadratic shape functions of SERENDIPITY type incorporating all layers. The nodes comprise enriched degrees of freedom to consider rotations and translations of the whole composite structure. A constant element edge of $h_\alpha^e = 10\,\mathrm{mm}\ \forall\ \alpha = \{1, 2\}$ is used at all subsequent studies to gain convergence and to sufficiently resolve the eigenmode. The discretisation strategy is visualised in Fig. 2 (top left) For comparison, identified ratios of our starting structure are: $TR = 0.15625$, $LR = 0.5$, $TLR = 9.136 \times 10^{-3}$, $GR = 9.978 \times 10^{-5}$, and $MDR = 0.384$. However, geometric and material parameters stated in Fig. 2 are varied systematically to analyse the mechanical eigenbehaviour for all possible values of these ratios, at least up to the bounds reported in Eqs. (1)–(5). The first natural frequency f_1 is used as evaluation criterion. Following dependencies can be expressed concerning geometric dimensions and material properties.